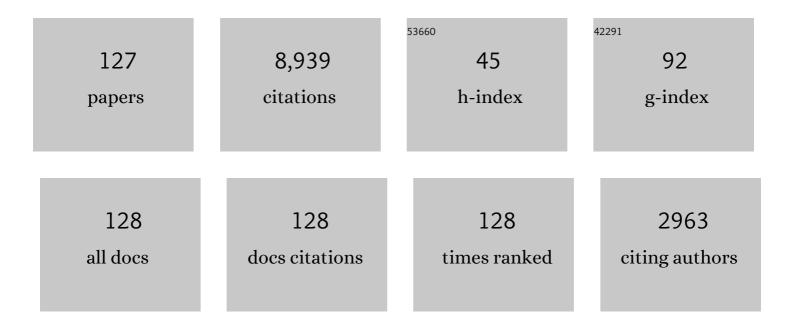
Ji-Feng Xu

List of Publications by Year in descending order

Source: https://exaly.com/author-pdf/2929497/publications.pdf Version: 2024-02-01



#	Article	IF	CITATIONS
1	Origin of the volcanic rocks in Dianzhong Formation, central Lhasa Terrane, Tibet: implication for the genesis of syn-collisional magmatism and Neo-Tethyan slab roll-back. International Geology Review, 2023, 65, 21-39.	1.1	6
2	Oxygen isotope heterogeneity of olivine crystals in orogenic peridotites from Songshugou, North Qinling Orogen: Petrogenesis and geodynamic implications. American Mineralogist, 2022, 107, 904-913.	0.9	2
3	Crustal reworking and growth during India–Asia continental collision: Insights from early Cenozoic granitoids in the central Lhasa Terrane, Tibet. Geological Journal, 2022, 57, 79-98.	0.6	1
4	Dupal Anomaly and Identification using Ndâ€Hf Isotopes. Acta Geologica Sinica, 2022, 96, 416-429.	0.8	0
5	In-situ mineralogical interpretation of the mantle geophysical signature of the Gangdese Cu-porphyry mineral system. Gondwana Research, 2022, 111, 53-63.	3.0	15
6	New geochronological and geochemical data for the Eocene shoshonitic trachyandesites in NW Iran: Constraints on their petrogenesis and tectonic setting. Lithos, 2022, , 106805.	0.6	0
7	<scp>Neoâ€Tethyan</scp> slab tearing constrained by Palaeocene <scp>Nâ€MORB</scp> â€like magmatism in southern Tibet. Geological Journal, 2021, 56, 205-223.	0.6	7
8	Early Cretaceous volcanic rocks in Yunzhug area, central Tibet, China, associated with arc–continent collision in the Tibetan Plateau?. Lithos, 2021, 380-381, 105827.	0.6	5
9	Lithospheric extension in response to subduction of the Paleo-Pacific Plate: Insights from Early Jurassic intraplate volcanic rocks in the Sk2 Borehole, Songliao Basin, NE China. Lithos, 2021, 380-381, 105871.	0.6	16
10	Negligible surface uplift following foundering of thickened central Tibetan lower crust. Geology, 2021, 49, 45-50.	2.0	25
11	Petrogenesis and metallogenesis of an extraordinary deeply hidden granite pluton overlain by W-Zn-Pb-Ag-mineralized roof: Example from Xidamingshan district, South China. Ore Geology Reviews, 2021, 130, 103932.	1.1	6
12	Early Cretaceous (â^¼138–134ÂMa) Forearc Ophiolite and Tectonomagmatic Patterns in Central Tibet: Subduction Termination and Reâ€initiation of Mesoâ€īethys Ocean Caused by Collision of an Oceanic Plateau at the Continental Margin?. Tectonics, 2021, 40, e2020TC006423.	1.3	22
13	Recycled volatiles determine fertility of porphyry deposits in collisional settings. American Mineralogist, 2021, 106, 656-661.	0.9	80
14	Molybdenum isotope systematics of subduction-related magmas from the Zhongdian region: Assessing the Mo fractionation behavior in magmatic-hydrothermal processes. Ore Geology Reviews, 2021, 133, 104089.	1.1	5
15	Long-lived low Th/U Pacific-type isotopic mantle domain: Constraints from Nd and Pb isotopes of the Paleo-Asian Ocean mantle. Earth and Planetary Science Letters, 2021, 567, 117006.	1.8	12
16	Late Eocene Two-Pyroxene Trachydacites from the Southern Qiangtang Terrane, Central Tibetan Plateau: High-Temperature Melting of Overthickened and Dehydrated Lower Crust. Journal of Petrology, 2021, 62, .	1.1	10
17	Early Mesozoic crustal evolution in the NW segment of West Qinling, China: Evidence from diverse intermediate–felsic igneous rocks. Lithos, 2021, 396-397, 106187.	0.6	5
18	Development of a complex arc–back-arc basin system within the South Tianshan Ocean: Insights from the Wuwamen ophiolitic peridotites. Lithos, 2021, , 106487.	0.6	0

#	Article	IF	CITATIONS
19	Geochemistry and Sr–Nd–Hf–Pb isotope systematics of late Carboniferous sanukitoids in northern West Junggar, NW China: Implications for initiation of ridge-subduction. Gondwana Research, 2021, 99, 204-218.	3.0	10
20	Late Cretaceous magmatism in the NW Lhasa Terrane, southern Tibet: Implications for crustal thickening and initial surface uplift. Bulletin of the Geological Society of America, 2020, 132, 334-352.	1.6	8
21	Petrogenesis of Early Jurassic (ca. 181ÂMa) dacitic–rhyolitic volcanic rocks in the Amdo ophiolite mélange, central Tibetan Plateau: Lowâ€pressure partial melts of Bangong–Nujiang Tethys oceanic crust?. Geological Journal, 2020, 55, 3283-3296.	0.6	7
22	Widespread Os-isotopically ultradepleted mantle domains in the Paleo-Asian oceanic upper mantle: evidence from the Paleozoic Tianshan ophiolites (NW China). International Journal of Earth Sciences, 2020, 109, 1421-1438.	0.9	5
23	Generation of the 105–100 Ma Dagze volcanic rocks in the north Lhasa Terrane by lower crustal melting at different temperature and depth: Implications for tectonic transition. Bulletin of the Geological Society of America, 2020, 132, 1257-1272.	1.6	26
24	Petrogenesis of Carboniferous volcanic rocks from the Gangou area, Chinese North Tianshan: Constraints on the evolution of the North Tianshan Ocean. Geological Journal, 2020, 55, 1931-1946.	0.6	2
25	"Garnet―Lherzolites in the Purang Ophiolite, Tibet: Evidence for Exhumation of Deep Oceanic Lithospheric Mantle. Geophysical Research Letters, 2020, 47, e2019GL086101.	1.5	18
26	The youngest Permian Ocean in Central Asian Orogenic Belt: Evidence from Geochronology and Geochemistry of Bingdaban Ophiolitic Mélange in Central Tianshan, northwestern China. Geological Journal, 2020, 55, 2062-2079.	0.6	19
27	Neoproterozoic active margin of the SW South China Block: Constraints from U Pb ages, Sr Nd isotopes and geochemical data for the gabbro and granodiorite along the Ailaoshan tectonic belt. Lithos, 2020, 358-359, 105387.	0.6	5
28	The genesis of felsic magmatism during the closure of the Northeastern Paleo-Tethys Ocean: Evidence from the Heri batholith in West Qinling, China. Gondwana Research, 2020, 84, 38-51.	3.0	19
29	Tectonic activities in Dongshangen polymetallic ore district, eastern Kunlun Mountains, Qinghai-Tibet Plateau: Evidences from fission track thermochronology. Ore Geology Reviews, 2019, 112, 103065.	1.1	10
30	Fluid flux in the lithosphere beneath southern Tibet during Neo-Tethyan slab breakoff: Evidence from an appinite–granite suite. Lithos, 2019, 344-345, 324-338.	0.6	38
31	Generation of coeval metaluminous and muscovite-bearing peraluminous granitoids in the same composite pluton in West Qinling, NE Tibetan Plateau. Lithos, 2019, 344-345, 374-392.	0.6	15
32	Geodynamic transition from subduction to extension: evidence from the geochronology and geochemistry of granitoids in the Sangsang area, southern Lhasa Terrane, Tibet. International Journal of Earth Sciences, 2019, 108, 1663-1681.	0.9	12
33	Highâ€Precision Measurement of ¹⁸⁷ Os/ ¹⁸⁸ Os Isotope Ratios of Nanogram to Picogram Amounts of Os in Geological Samples by Nâ€ <scp>TIMS</scp> using Faraday Cups Equipped with 10 ¹³ Ω Amplifiers. Geostandards and Geoanalytical Research, 2019, 43, 419-433.	1.7	9
34	Geology and Genesis of the Giant Pulang Porphyry Cu-Au District, Yunnan, Southwest China. Economic Geology, 2019, 114, 275-301.	1.8	42
35	Initial Rifting of the Lhasa Terrane from Gondwana: Insights From the Permian (~262ÂMa) Amphiboleâ€Rich Lithospheric Mantleâ€Derived Yawa Basanitic Intrusions in Southern Tibet. Journal of Geophysical Research: Solid Earth, 2019, 124, 2564-2581.	1.4	54
36	Breakup of Eastern Gondwana as inferred from the Lower Cretaceous Charong Dolerites in the central Tethyan Himalaya, southern Tibet. Palaeogeography, Palaeoclimatology, Palaeoecology, 2019, 515, 70-82.	1.0	17

#	Article	IF	CITATIONS
37	Evolution of the northward subduction of the Neo-Tethys: Implications of geochemistry of Cretaceous arc volcanics in Qinghai-Tibetan Plateau. Palaeogeography, Palaeoclimatology, Palaeoecology, 2019, 515, 83-94.	1.0	11
38	Origin of dioritic magma and its contribution to porphyry Cu–Au mineralization at Pulang in the Yidun arc, eastern Tibet. Lithos, 2018, 304-307, 436-449.	0.6	38
39	A new method for calibrating the current gain of 10 ¹³ Ω amplifiers in thermal ionization mass spectrometry. Journal of Mass Spectrometry, 2018, 53, 455-464.	0.7	5
40	Geochronological and geochemical constraints on the origin of the Yunzhug ophiolite in the Shiquanhe–Yunzhug–Namu Tso ophiolite belt, Lhasa Terrane, Tibetan Plateau. Lithos, 2018, 300-301, 250-260.	0.6	59
41	Late Cenozoic magmatic inflation, crustal thickening, and >2 km of surface uplift in central Tibet. Geology, 2018, 46, 19-22.	2.0	53
42	Petrogenesis and geodynamic significance of Neoproterozoic (â^¼925â€⁻Ma) high-Fe–Ti gabbros of the RenTso ophiolite, Lhasa Terrane, central Tibet. Precambrian Research, 2018, 314, 160-169.	1.2	12
43	Origin of Miocene Cu-bearing porphyries in the Zhunuo region of the southern Lhasa subterrane: Constraints from geochronology and geochemistry. Gondwana Research, 2017, 41, 51-64.	3.0	41
44	New precise zircon U-Pb and muscovite 40 Ar- 39 Ar geochronology of the Late Cretaceous W-Sn mineralization in the Shanhu orefield, South China. Ore Geology Reviews, 2017, 84, 338-346.	1.1	16
45	Re–Os isotope evidence from Mesozoic and Cenozoic basalts for secular evolution of the mantle beneath the North China Craton. Contributions To Mineralogy and Petrology, 2017, 172, 1.	1.2	18
46	ldentification of an Early–Middle Jurassic oxidized magmatic belt, south Gangdese, Tibet, and geological implications. Science Bulletin, 2017, 62, 888-898.	4.3	19
47	Geochemical signature and rock associations of ocean ridge-subduction: Evidence from the Karamaili Paleo-Asian ophiolite in east Junggar, NW China. Gondwana Research, 2017, 48, 34-49.	3.0	47
48	Late Triassic E-MORB-like basalts associated with porphyry Cu-deposits in the southern Yidun continental arc, eastern Tibet: Evidence of slab-tear during subduction?. Ore Geology Reviews, 2017, 90, 1054-1062.	1.1	37
49	Slab Breakoff of the Neoâ€Tethys Ocean in the Lhasa Terrane Inferred From Contemporaneous Melting of the Mantle and Crust. Geochemistry, Geophysics, Geosystems, 2017, 18, 4074-4095.	1.0	41
50	A comparison using Faraday cups with 10 ¹³ Ω amplifiers and a secondary electron multiplier to measure Os isotopes by negative thermal ionization mass spectrometry. Rapid Communications in Mass Spectrometry, 2017, 31, 1616-1622.	0.7	12
51	Precise and accurate Re–Os isotope dating of organic-rich sedimentary rocks by thermal ionization mass spectrometry with an improved H2O2-HNO3 digestion procedure. International Journal of Mass Spectrometry, 2017, 421, 263-270.	0.7	14
52	Early paleozoic granodioritic plutons in the Shedong W–Mo ore district, Guangxi, southern China: Products of re-melting of middle Proterozoic crust due to magma underplating. Journal of Asian Earth Sciences, 2017, 141, 59-73.	1.0	17
53	Sedimentary record of Jurassic northward subduction of the Bangong–Nujiang Ocean: insights from detrital zircons. International Geology Review, 2017, 59, 166-184.	1.1	68
54	High-Al and high-Cr podiform chromitites from the western Yarlung-Zangbo suture zone, Tibet: Implications from mineralogy and geochemistry of chromian spinel, and platinum-group elements. Ore Geology Reviews, 2017, 80, 1020-1041.	1.1	41

#	Article	IF	CITATIONS
55	Origin of Permian extremely high Ti/Y mafic lavas and dykes from Western Guangxi, SW China: Implications for the Emeishan mantle plume magmatism. Journal of Asian Earth Sciences, 2017, 141, 97-111.	1.0	26
56	Molybdenum Mass Fractions and Isotopic Compositions of International Geological Reference Materials. Geostandards and Geoanalytical Research, 2016, 40, 217-226.	1.7	72
57	Oxygen isotope and trace element geochemistry of zircons from porphyry copper system: Implications for Late Triassic metallogenesis within the Yidun Terrane, southeastern Tibetan Plateau. Chemical Geology, 2016, 441, 148-161.	1.4	35
58	Sediment melting during subduction initiation: Geochronological and geochemical evidence from the <scp>D</scp> arutso highâ€ <scp>M</scp> g andesites within ophiolite melange, central <scp>T</scp> ibet. Geochemistry, Geophysics, Geosystems, 2016, 17, 4859-4877.	1.0	98
59	Discovery of eclogite in the Bangong Co–Nujiang ophiolitic mélange, central Tibet, and tectonic implications. Gondwana Research, 2016, 35, 115-123.	3.0	28
60	Optimization techniques for improving the precision of isotopic analysis by thermal ionization mass spectrometry, taking strontium, neodymium, lead, and osmium as examples. Spectroscopy Letters, 2016, 49, 85-90.	0.5	4
61	Double-layer structure of the crust beneath the Zhongdian arc, SW China: U–Pb geochronology and Hf isotope evidence. Journal of Asian Earth Sciences, 2016, 115, 455-467.	1.0	45
62	Two Cenozoic tectonic events of N–S and E–W extension in the Lhasa Terrane: Evidence from geology and geochronology. Lithos, 2016, 245, 118-132.	0.6	26
63	Decadal variability in seawater p <scp>H</scp> in the <scp>W</scp> est <scp>P</scp> acific: Evidence from coral Î ¹¹ <scp>B</scp> records. Journal of Geophysical Research: Oceans, 2015, 120, 7166-7181.	1.0	22
64	Os–Nd–Sr isotopes in Miocene ultrapotassic rocks of southern Tibet: Partial melting of a pyroxenite-bearing lithospheric mantle?. Geochimica Et Cosmochimica Acta, 2015, 163, 279-298.	1.6	53
65	Geochemical differences between subduction- and collision-related copper-bearing porphyries and implications for metallogenesis. Ore Geology Reviews, 2015, 70, 424-437.	1.1	25
66	Electron microprobe analyses of ore minerals and H–O, S isotope geochemistry of the Yuerya gold deposit, eastern Hebei, China: Implications for ore genesis and mineralization. Ore Geology Reviews, 2015, 69, 199-216.	1.1	14
67	Late Cretaceous high-Mg# granitoids in southern Tibet: Implications for the early crustal thickening and tectonic evolution of the Tibetan Plateau?. Lithos, 2015, 232, 12-22.	0.6	48
68	Disequilibrium-induced initial Os isotopic heterogeneity in gram aliquots of single basaltic rock powders: Implications for dating and source tracing. Chemical Geology, 2015, 406, 10-17.	1.4	27
69	The boundary between the Central Asian Orogenic belt and Tethyan tectonic domain deduced from Pb isotopic data. Journal of Asian Earth Sciences, 2015, 113, 7-15.	1.0	19
70	Identifying mantle carbonatite metasomatism through Os–Sr–Mg isotopes in Tibetan ultrapotassic rocks. Earth and Planetary Science Letters, 2015, 430, 458-469.	1.8	82
71	Evidence for crustal contamination in intra-continental OIB-like basalts from West Qinling, central China: A Re–Os perspective. Journal of Asian Earth Sciences, 2015, 98, 436-445.	1.0	8
72	Reassessment of Hydrofluoric Acid Desilicification in the Carius Tube Digestion Technique for Re–Os Isotopic Determination in Geological Samples. Geostandards and Geoanalytical Research, 2015, 39, 17-30.	1.7	52

#	Article	IF	CITATIONS
73	Petrological and Os isotopic constraints on the origin of the Dongbo peridotite massif, Yarlung Zangbo Suture Zone, Western Tibet. Journal of Asian Earth Sciences, 2015, 110, 72-84.	1.0	29
74	Re–Os isotope and platinum-group element geochemistry of the Pobei Ni–Cu sulfide-bearing mafic–ultramafic complex in the northeastern part of the Tarim Craton. Mineralium Deposita, 2014, 49, 381-397.	1.7	23
75	Geochronology and geochemistry of the Sangri Group Volcanic Rocks, Southern Lhasa Terrane: Implications for the early subduction history of the Neo-Tethys and Gangdese Magmatic Arc. Lithos, 2014, 200-201, 157-168.	0.6	177
76	Geochemical and Sr–Nd–Pb–Os isotopic compositions of Miocene ultrapotassic rocks in southern Tibet: Petrogenesis and implications for the regional tectonic history. Lithos, 2014, 208-209, 237-250.	0.6	42
77	A method for determination of PGE–Re concentrations and Os isotopic compositions in environmental materials. Analytical Methods, 2014, 6, 5537.	1.3	6
78	Measurement of the Isotopic Composition of Molybdenum in Geological Samples by MCâ€ICPâ€MS using a Novel Chromatographic Extraction Technique. Geostandards and Geoanalytical Research, 2014, 38, 345-354.	1.7	90
79	Isotope studies of human remains from Mayutian, Yunnan Province, China. Journal of Archaeological Science, 2014, 50, 414-419.	1.2	14
80	Geology and origin of the post-collisional Narigongma porphyry Cu–Mo deposit, southern Qinghai, Tibet. Gondwana Research, 2014, 26, 536-556.	3.0	60
81	The Dupal isotopic anomaly in the southern Paleo-Asian Ocean: Nd–Pb isotope evidence from ophiolites in Northwest China. Lithos, 2014, 189, 185-200.	0.6	48
82	Chalcophile elemental compositions of MORBs from the ultraslow-spreading Southwest Indian Ridge and controls of lithospheric structure on S-saturated differentiation. Chemical Geology, 2014, 382, 1-13.	1.4	35
83	Chemical heterogeneity of the Emeishan mantle plume: Evidence from highly siderophile element abundances in picrites. Journal of Asian Earth Sciences, 2014, 79, 191-205.	1.0	14
84	Geochronology and geochemical characteristics of Late Triassic porphyritic rocks from the Zhongdian arc, eastern Tibet, and their tectonic and metallogenic implications. Gondwana Research, 2014, 26, 492-504.	3.0	66
85	Determination of Platinumâ€Group Elements and <scp>R</scp> eâ€ <scp>O</scp> s Isotopes using <scp>ID</scp> â€ <scp>ICP</scp> â€ <scp>MS</scp> and Nâ€ <scp>TIMS</scp> from a Single Digestion after Two‧tage Column Separation. Geostandards and Geoanalytical Research, 2014, 38, 37-50.	1.7	72
86	Geochronological, geochemical and Nd–Hf–Os isotopic fingerprinting of an early Neoproterozoic arc–back-arc system in South China and its accretionary assembly along the margin of Rodinia. Precambrian Research, 2013, 231, 343-371.	1.2	218
87	Cenozoic Mg-rich potassic rocks in the Tibetan Plateau: Geochemical variations, heterogeneity of subcontinental lithospheric mantle and tectonic implications. Journal of Asian Earth Sciences, 2012, 53, 115-130.	1.0	34
88	Geochemistry of Miocene trachytes in Bugasi, Lhasa block, Tibetan Plateau: Mixing products between mantle- and crust-derived melts?. Gondwana Research, 2012, 21, 112-122.	3.0	40
89	Geochemical variations in Miocene adakitic rocks from the western and eastern Lhasa terrane: Implications for lower crustal flow beneath the Southern Tibetan Plateau. Lithos, 2011, 125, 928-939.	0.6	73
90	Simplified technique for the measurements of Re-Os isotope by multicollector inductively coupled plasma mass spectrometry (MC-ICP-MS). Geochemical Journal, 2010, 44, 73-80.	0.5	39

(

#	Article	IF	CITATIONS
91	Evolution of the Lüliangshan garnet peridotites in the North Qaidam UHP belt, Northern Tibetan Plateau: Constraints from Re–Os isotopes. Lithos, 2010, 117, 307-321.	0.6	31
92	Os, Nd and Sr isotope and trace element geochemistry of the Muli picrites: Insights into the mantle source of the Emeishan Large Igneous Province. Lithos, 2010, 119, 108-122.	0.6	75
93	Presence of Permian extension- and arc-type magmatism in southern Tibet: Paleogeographic implications. Bulletin of the Geological Society of America, 2010, 122, 979-993.	1.6	167
94	Origin of Cenozoic alkaline potassic volcanic rocks at KonglongXiang, Lhasa terrane, Tibetan Plateau: Products of partial melting of a mafic lower-crustal source?. Chemical Geology, 2010, 273, 286-299.	1.4	121
95	Determination of rhenium content in molybdenite by ICP–MS after separation of the major matrix by solvent extraction with N-benzoyl-N-phenylhydroxalamine. Talanta, 2010, 81, 954-958.	2.9	23
96	Triassic Nb-enriched basalts, magnesian andesites, and adakites of the Qiangtang terrane (Central) Tj ETQq0 0 0 Mineralogy and Petrology, 2008, 155, 473-490.	rgBT /Ove 1.2	erlock 10 Tf 5 185
97	Geochemistry of the Mian-Lue ophiolites in the Qinling Mountains, central China: Constraints on the evolution of the Qinling orogenic belt and collision of the North and South China Cratons. Journal of Asian Earth Sciences, 2008, 32, 336-347.	1.0	35
98	Eocene melting of subducting continental crust and early uplifting of central Tibet: Evidence from central-western Qiangtang high-K calc-alkaline andesites, dacites and rhyolites. Earth and Planetary Science Letters, 2008, 272, 158-171.	1.8	320
99	Partial Melting of Thickened or Delaminated Lower Crust in the Middle of Eastern China: Implications for Cuâ€Au Mineralization. Journal of Geology, 2007, 115, 149-161.	0.7	164
100	Petrogenesis of Carboniferous adakites and Nb-enriched arc basalts in the Alataw area, northern Tianshan Range (western China): Implications for Phanerozoic crustal growth in the Central Asia orogenic belt. Chemical Geology, 2007, 236, 42-64.	1.4	216
101	Os, Pb, and Nd isotope geochemistry of the Permian Emeishan continental flood basalts: Insights into the source of a large igneous province. Geochimica Et Cosmochimica Acta, 2007, 71, 2104-2119.	1.6	109
102	Early Cretaceous adakitic granites in the Northern Dabie Complex, central China: Implications for partial melting and delamination of thickened lower crust. Geochimica Et Cosmochimica Acta, 2007, 71, 2609-2636.	1.6	446
103	Identification of mantle plumes in the Emeishan Large Igneous Province. Episodes, 2007, 30, 32-42.	0.8	63
104	Petrogenesis of Adakitic Porphyries in an Extensional Tectonic Setting, Dexing, South China: Implications for the Genesis of Porphyry Copper Mineralization. Journal of Petrology, 2006, 47, 119-144.	1.1	723
105	Na depletion in modern adakites via melt/rock reaction within the sub-arc mantle. Chemical Geology, 2006, 229, 273-292.	1.4	62
106	Petrogenesis of Cretaceous adakitic and shoshonitic igneous rocks in the Luzong area, Anhui Province (eastern China): Implications for geodynamics and Cu–Au mineralization. Lithos, 2006, 89, 424-446.	0.6	409
107	Cenozoic K-rich adakitic volcanic rocks in the Hohxil area, northern Tibet: Lower-crustal melting in an intracontinental setting. Geology, 2005, 33, 465.	2.0	394
108	Alkaline syenites in eastern Cathaysia (South China): link to Permian–Triassic transtension. Earth and Planetary Science Letters, 2005, 230, 339-354.	1.8	195

#	Article	IF	CITATIONS
109	Geochemistry and Petrogenesis of the Tongshankou and Yinzu Adakitic Intrusive Rocks and the Associated Porphyry Copperâ€Molybdenum Mineralization in Southeast Hubei, East China. Resource Geology, 2004, 54, 137-152.	0.3	119
110	Crust-mantle interaction during the tectono-thermal reactivation of the North China Craton: constraints from SHRIMP zircon U–Pb chronology and geochemistry of Mesozoic plutons from western Shandong. Contributions To Mineralogy and Petrology, 2004, 147, 750-767.	1.2	279
111	Geochemical and Nd–Pb isotopic characteristics of the Tethyan asthenosphere: implications for the origin of the Indian Ocean mantle domain. Tectonophysics, 2004, 393, 9-27.	0.9	295
112	Cretaceous high-potassium intrusive rocks in the Yueshan-Hongzhen area of east China: Adakites in an extensional tectonic regime within a continent. Geochemical Journal, 2004, 38, 417-434.	0.5	188
113	Petrogenesis of the Mesozoic intrusive rocks in the Tongling area, Anhui Province, China and their constraint on geodynamic process. Science in China Series D: Earth Sciences, 2003, 46, 801-815.	0.9	60
114	Carboniferous adakites and Nb-enriched arc basaltic rocks association in the Alataw Mountains, north Xinjiang: interactions between slab melt and mantle peridotite and implications for crustal growth. Science Bulletin, 2003, 48, 2108-2115.	1.7	19
115	Origin of two differentiation trends in the Emeishan flood basalts. Science Bulletin, 2003, 48, 390-394.	1.7	23
116	Geochemistry of late Paleozoic mafic igneous rocks from the Kuerti area, Xinjiang, northwest China: implications for backarc mantle evolution. Chemical Geology, 2003, 193, 137-154.	1.4	146
117	Extremely high-Na adakite-like magmas derived from alkali-rich basaltic underplate: The Late Cretaceous Zhantang andesites in the Huichang Basin, SE China Geochemical Journal, 2003, 37, 233-252.	0.5	89
118	Petrogenesis of the Mesozoic intrusive rocks in the Tongling area, Anhui Province, China and their constraint on geodynamic process. Science in China Series D: Earth Sciences, 2003, 46, 801.	0.9	1
119	Origin of Mesozoic adakitic intrusive rocks in the Ningzhen area of east China: Partial melting of delaminated lower continental crust?. Geology, 2002, 30, 1111.	2.0	817
120	MORB-type rocks from the Paleo-Tethyan Mian-Lueyang northern ophiolite in the Qinling Mountains, central China: implications for the source of the low 206Pb/204Pb and high 143Nd/144Nd mantle component in the Indian Ocean. Earth and Planetary Science Letters, 2002, 198, 323-337.	1.8	143
121	Adakites related to subduction in the northern margin of Junggar arc for the Late Paleozoic: Products of slab melting. Science Bulletin, 2001, 46, 1312-1316.	1.7	36
122	Adakite-type sodium-rich rocks in Awulale Mountain of west Tianshan: Significance for the vertical growth of continental crust. Science Bulletin, 2001, 46, 811-817.	1.7	25
123	Geochemistry of high-Mg andesites and adakitic andesite from the Sanchazi block of the Mian-Lue ophiolitic melange in the Qinling Mountains, central China: Evidence of partial melting of the subducted Paleo-Tethyan crust Geochemical Journal, 2000, 34, 359-377.	0.5	58
124	The recognition of adakite-type gneisses in the North Dabie Mountain and its implication to ultrahigh pressure metamorphic geology. Science Bulletin, 2000, 45, 1927-1933.	1.7	6
125	Discovery of Mg-righ volcanic rock series in western Altay area, Xinjiang and its geologic significance. Science Bulletin, 1999, 44, 1685-1688.	1.7	27
126	Discovery of the highly depleted N-MORB-type volcanic rocks: new evidence for the Mianlue paleo-ocean. Science Bulletin, 1998, 43, 510-514.	1.7	17

#	Article	IF	CITATIONS
127	Magmatic record of continuous Neo-Tethyan subduction after initial India-Asia collision in the central part of southern Tibet. Bulletin of the Geological Society of America, 0, , .	1.6	7